



Interannual variability in the longitudinal structure of the low-latitude ionosphere due to the El Niño–Southern Oscillation

N. M. Pedatella¹ and J. M. Forbes¹

Received 27 May 2009; revised 14 September 2009; accepted 22 September 2009; published 22 December 2009.

[1] The ratio of monthly median f_oF_2 values between the ionosondes at Maui (20.8°N, −156°E geographic; 21.2°N, −90.4°E geomagnetic) and Yamagawa (31.2°N, 130.6°E geographic; 20.6°N, −160.9°E geomagnetic) from January 1960 to June 1993 are used to investigate interannual variability in the wave-4 longitudinal structure of the low-latitude F region ionosphere. Analysis of Global Positioning System total electron content between January 1998 and December 2008 reveals that the ratio between these two locations is a suitable proxy for the amplitude of the wave-4 longitudinal structure in the Northern Hemisphere. Significant interannual variability is present in the f_oF_2 ratio after removing the solar cycle and intra-annual variability. The remaining variability is thought to be due, in part, to changes in atmospheric and oceanic circulations arising from the El Niño–Southern Oscillation (ENSO). Wavelet analysis reveals that similar periodicities and occurrence times exist for the f_oF_2 ratio monthly anomalies and sea surface temperature anomalies, represented by the Oceanic Niño Index (ONI). Furthermore, the yearly ONI extreme value is well correlated with the extreme value of the f_oF_2 ratio monthly anomalies in the subsequent 5 months. This surprising connection is attributed to changes in tropospheric convection, and hence latent heating, associated with changing sea surface temperatures due to the ENSO. Changing distributions of latent heat tidal forcing are thought to induce changes in the strength of the upward and eastward propagating diurnal tide with zonal wave number $s = -3$ (DE3) which subsequently produces the observed changes in the amplitude of the wave-4 longitudinal structure through modulation of the electric fields generated by the dynamo mechanism in the ionospheric E region. Our results demonstrate that there is significant interannual variability in the ionospheric wave-4 longitudinal structure and further indicate that the ENSO phenomenon represents a source of ionospheric variability which has previously not been considered.

Citation: Pedatella, N. M., and J. M. Forbes (2009), Interannual variability in the longitudinal structure of the low-latitude ionosphere due to the El Niño–Southern Oscillation, *J. Geophys. Res.*, *114*, A12316, doi:10.1029/2009JA014494.

1. Introduction

[2] At low latitudes, the F region electron density maxima are located 10–20° to the north and south of the geomagnetic equator. This feature is known as the equatorial ionization anomaly (EIA) and is due to the eastward direction of the daytime E region electric fields that are generated by neutral winds through the dynamo mechanism. At low latitudes, the daytime eastward electric field results in a vertical $\mathbf{E} \times \mathbf{B}$ drift and an uplift of the ionospheric plasma. Subsequent motion under the gravitational force results in the plasma traveling downward along the magnetic field lines and

being deposited at locations north and south of the magnetic equator [Appleton, 1946].

[3] A number of observational studies have demonstrated the dominance of a zonal wave number-4 (hereafter called wave-4) longitudinal structure in the EIA when viewed at a fixed local time. The wave-4 structure has been observed in Far Ultraviolet images [Sagawa *et al.*, 2005; Immel *et al.*, 2006], total electron content (TEC) [Scherliess *et al.*, 2008; Wan *et al.*, 2008], ionospheric peak height [Lin *et al.*, 2007], and F region electron densities [Kil *et al.*, 2007; Liu and Watanabe, 2008]. Although the role of neutral winds in generating the EIA has long been recognized, Immel *et al.* [2006] were the first to connect the longitudinal structures in the EIA with variations in the strength of neutral winds due to upward propagating tides. The predominant origin of the wave-4 structure appears to be the eastward propagating diurnal tide with zonal wave number $s = -3$ [Hagan *et al.*, 2007], often referred to as DE3. DE3 is generated by the

¹Department of Aerospace Engineering Sciences, University of Colorado, Boulder, Colorado, USA.

longitude dependence of latent heating due to deep convection in the tropics [Hagan and Forbes, 2002; Forbes et al., 2001, 2006; Oberheide et al., 2006]. DE3 propagates vertically and modulates the E region electric fields that are generated through the dynamo mechanism. Wave-4 longitudinal structures observed in the equatorial electrojet [Lühr et al., 2008] and in $\mathbf{E} \times \mathbf{B}$ drift velocities [Kil et al., 2007; Hartman and Heelis, 2007] provide observational evidence for the modulation of E region electric fields by DE3. Since the E region electric fields are responsible for the strength and formation of the EIA, variations in the strength of the E region electric fields due to DE3 produces a wave-4 longitudinal structure in the EIA.

[4] DE3 exhibits significant intra-annual variability, and it achieves maximum amplitude in August–September and is minimum during December–January [Oberheide et al., 2006; Forbes et al., 2008]. Similar intra-annual variability has been observed in the wave-4 longitudinal structure of the low-latitude ionosphere [England et al., 2009; Liu and Watanabe, 2008; Wan et al., 2008]. These prior studies demonstrate that changes in the amplitude of DE3 impact the formation and strength of the wave-4 longitudinal structure observed in the low-latitude ionosphere. However, they have only addressed the question of how the intra-annual variability in the wave-4 longitudinal structure is related to the intra-annual variability of the DE3 amplitude in a climatological sense. Although DE3 exhibits significant intra-annual variability, DE3 and other nonmigrating tides can also experience day-to-day and interannual variability. Interannual variability in the strength of DE3 was observed by Forbes et al. [2008]; however, the cause of this variability is unknown. Day-to-day variability in the amplitude of DE3 is closely related with temporal variations in tropical rainfall [Miyoshi, 2006]. Because of the large-scale changes in precipitation and surface temperatures associated with the El Niño–Southern Oscillation (ENSO) [Ropelewski and Halpert, 1987; Trenberth et al., 2002], it is not surprising that interannual variability in DE3, and other nonmigrating tides, is associated with the ENSO. Gurubaran et al. [2005] observed a decrease in the amplitude of the diurnal tide at mesopause altitudes and attributed this to an increase in the strength of nonmigrating tides associated with the ENSO. During the 1997–1998 El Niño event, Lieberman et al. [2007] observed large changes in tidal amplitudes due to latent heating in the equatorial region. They reported equatorial increases in DE1 and DW3 and a decrease in the equatorial amplitude of DE3. Given the connection between the amplitude of DE3 and the ionospheric wave-4 longitudinal structure along with the possible interannual variability in the amplitude of nonmigrating tides due to the ENSO, interannual variability might therefore be expected in the amplitude of the wave-4 longitudinal structure.

[5] The primary aim of the present study is to explore interannual variability in the wave-4 longitudinal structure of the low-latitude ionosphere and its connection to changes in atmospheric and oceanic circulation resulting from the ENSO. Prior studies on longitudinal structures in the low-latitude ionosphere have relied upon either satellite-based measurements [Immel et al., 2006; Lin et al., 2007; Liu and Watanabe, 2008; Pedatella et al., 2008; Scherliess et al., 2008] or Global Positioning System (GPS) TEC observations [Wan et al., 2008]. The combination of limited local

time sampling and the relatively short time series available from these observation methods make them ill suited for studying the interannual variability of the wave-4 longitudinal structure. We thus use the ratio of monthly median f_oF_2 values between two ionosonde stations from January 1960 to June 1993 as a proxy for the strength of the wave-4 longitudinal structure. Analysis of GPS TEC reveals that the ratio of ionospheric parameters between two locations is a suitable means for assessing the strength of the wave-4 longitudinal structure in the Northern Hemisphere. This is the first time that interannual variability of the wave-4 longitudinal structure has been addressed. Furthermore, we present evidence that the ENSO represents a source of ionospheric variability which has previously not been considered.

2. Data and Methods

2.1. Ionosonde Observations

[6] For the present study we use monthly median f_oF_2 observations during 1500–1600 LT at the ionosonde stations located at Maui (20.8°N, –156°E geographic; 21.2°N, –90.4°E geomagnetic) and Yamagawa (31.2°N, 130.6°E geographic; 20.6°N, –160.9°E geomagnetic). Local times of 15–16 h are used in the present analysis since the EIA and wave-4 structure are well established during this time. Data from January 1960 to June 1993 for these two ionosonde stations are available through the National Geophysical Data Center Space Physics Interactive Data Resource (available at <http://spidr.ngdc.noaa.gov>). The location of these two ionosonde stations along with the monthly median GPS TEC between 1500 and 1600 LT during August 2008 is presented in Figure 1. The monthly median GPS TEC data presented in Figure 1 are based on the daily global ionosphere maps (GIMs) during August 2008 produced by the International GNSS Service (IGS) [Dow et al., 2005] (additional details on the GPS TEC processing are provided in section 2.2). The global wave-4 longitudinal structure in the August 2008 monthly median GPS TEC can clearly be observed. Figure 1 also shows that the Maui ionosonde is located in a longitude sector of enhanced EIA strength while the Yamagawa ionosonde is located near a minimum in the strength of the EIA associated with the wave-4 structure. Because of the location of the ionosonde stations with respect to the longitude sectors of maximum and minimum EIA and wave-4 strength, the monthly median f_oF_2 at Maui is divided by the corresponding value at Yamagawa to obtain a time series of f_oF_2 ratio that is representative of the strength of the wave-4 longitudinal structure. The use of the f_oF_2 ratio as a proxy for the wave-4 structure is validated using GPS TEC observations, and further details on this relationship are presented in section 3.

[7] As the present study is focused on interannual variability in the ionospheric wave-4 longitudinal structure, we first remove the known variability from the f_oF_2 ratio time series. The wave-4 longitudinal structure around a local time of noon exhibits a solar cycle dependence that is inversely related to solar activity [Liu and Watanabe, 2008]. To remove the solar cycle variability, a least squares regression analysis was performed on the f_oF_2 ratio time series. The regression included a constant term and periodic

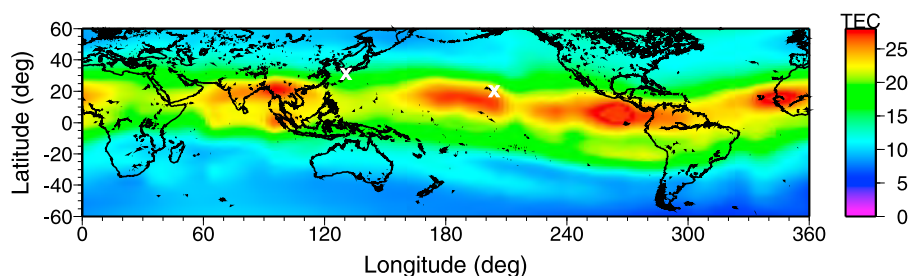


Figure 1. Median GPS TEC in August 2008 and the location of the ionosonde stations in Maui and Yamagawa (white crosses).

terms with periods of 10.28 years and 7.86 years. These periodicities correspond to the two dominant periodicities in both the f_oF_2 ratio and the $F_{10.7}$ cm solar radio flux during the time period of January 1960 to June 1993. It should be noted that the 10.28 year period is significantly stronger than the 7.86 year period; however, the inclusion of the two most dominant periods was necessary to adequately fit the data. The residuals from the regression analysis were then used for the subsequent analysis. Significant intra-annual variability also exists in the strength of the wave-4 longitudinal structure [England *et al.*, 2009; Liu and Watanabe, 2008; Scherliess *et al.*, 2008; Wan *et al.*, 2008]. Using the residuals from the solar cycle fit the intra-annual f_oF_2 ratio climatology is obtained by computing a mean value for each month. The climatological monthly mean values are then subtracted from the solar cycle fit residuals in order to obtain a time series of f_oF_2 ratio monthly anomalies (RMAs). The greater than 40 years of f_oF_2 RMAs provide the extended time series that is desired for the exploration of interannual variability in the wave-4 longitude structure.

2.2. Global Positioning System Total Electron Content

[8] GPS TEC is a column integral measurement of the electron density from the surface of the Earth to $\sim 20,200$ km; however, it is primarily dominated by F region electron densities [Klobuchar, 1996]. Therefore, GPS TEC observations can be considered to be proportional to f_oF_2 , and we analyze GPS TEC observations in order to validate the use of the f_oF_2 ratio between the two ionosonde stations as a proxy for the wave-4 longitudinal structure. The GPS TEC measurements come from the IGS GIMs [Dow *et al.*, 2005] and are based on slant TEC measurements from a global network of around 200 GPS receivers [Mannucci *et al.*, 1998]. The GIMs have a spatial resolution of 2.5° in latitude and 5° in longitude and a temporal resolution of 2 h. The daily GIMs are used to create monthly median GIMs from January 1999 to December 2008. The monthly median TEC observations between 10°N and 20°N magnetic latitude are first normalized by the zonal mean TEC and then a least squares fit to wave numbers 0–6 is performed to determine the amplitude and phase of each component. The amplitude of the wave number-4 component is then used in the subsequent analysis. Since the ionosondes are located in the Northern Hemisphere, we have focused only on the longitudinal structure in the northern EIA region due to the possibility of hemispheric asymmetries [McDonald *et al.*, 2008]. The ratio of the monthly median TEC between 20°N , -155°E and 30°N , 130°E geographic is also computed. The solar cycle and

intra-annual variability is removed from the time series of GPS TEC wave-4 amplitude and GPS TEC ratio to obtain a time series of monthly anomalies in the same manner as was done for the ionosonde observations. To illustrate the use of the f_oF_2 ratio as a suitable proxy for the wave-4 amplitude, a comparison of the GPS TEC wave-4 amplitude and GPS TEC ratio monthly anomalies has been performed, the results of which are presented in section 3.

2.3. Oceanic Niño Index

[9] In the present analysis the ENSO variability is represented by the Oceanic Niño Index (ONI). The ONI is a 3 month running mean of the version 3b extended reconstructed sea surface temperature (SST) anomalies [Xue *et al.*, 2003; Smith *et al.*, 2008] in the Niño 3.4 region (-5°N , 120°W). Values of ONI are available through the National Oceanic and Atmospheric Administration (NOAA) climate prediction center (available at <http://www.cpc.noaa.gov>). The ONI is used by NOAA for the identification of El Niño and La Niña events. El Niño time periods are associated with an increase in SSTs in the tropical Pacific and thus positive values of the ONI. Likewise, negative values of the ONI occur during La Niña time periods. El Niño and La Niña events influence the large-scale atmospheric circulation in different ways, and the ONI provides a useful index for tracking these changes.

3. Results and Discussion

[10] Monthly anomalies from January 1999 to December 2008 for GPS TEC ratio and the GPS TEC–based wave-4 amplitude are shown in Figure 2. The correlation coefficient between the two time series is 0.63 indicating reasonably good agreement. Although there are some discrepancies, the general trends in the GPS TEC ratio and the wave-4 amplitude in the Northern Hemisphere are similar. For example, both show anomalously high values during December–February during the initial portion of the time interval and then during July–September in 2006–2008. The slight discrepancy between the GPS TEC ratio monthly anomalies and the wave-4 amplitude monthly anomalies may be due to any changes in the location of the longitudinal sectors where the wave-like structure attains maximum amplitude. Removing the climatological monthly mean values eliminates the error due to the ionosphere changing from a wave-4 structure during March to October/November to a wave-3 structure in November/December. However, if the longitudinal structure shifts eastward or westward for a

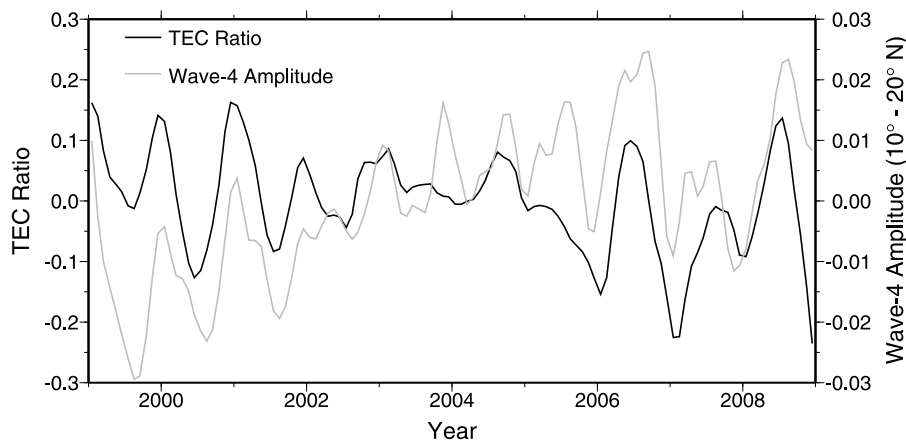


Figure 2. Monthly GPS TEC ratio anomalies (black) and the GPS TEC wave-4 amplitude between 10 and 20°N magnetic latitude (grey).

short time period then the TEC ratio may not be in agreement with the wave-4 amplitude.

[11] Given the general agreement between the GPS TEC ratio and the wave-4 amplitude monthly anomalies the ratio between the Maui and Yamagawa monthly median f_oF_2 ratios are judged to represent a suitable proxy for the amplitude of the wave-4 longitudinal structure. Unfortunately, because of a lack of overlap between the two time series, it is not possible to directly compare the f_oF_2 RMAs with the wave-4 amplitude as derived from GPS TEC observations. The ratio of the monthly median f_oF_2 values from January 1960 to June 1993 is shown in Figure 3 along with the solar cycle fit and the 81 day smoothed $F_{10.7}$ cm solar radio flux. The solar cycle and intra-annual variability is clearly observed in the f_oF_2 ratio values. It is interesting that the amplitude of the wave-4 structure is anticorrelated with solar activity which is consistent with previous observations [Liu and Watanabe, 2008]. This dependence on solar activity is due, at least in part, to the way that molecular dissipation affects the vertical propagation of DE3, through the temperature dependence of molecular viscosity and conductivity, and the dependence of wave vertical structure

on the ratio between wave vertical wavelength and the density-scale height [Forbes and Garrett, 1979; Lindzen, 1970; Oberheide et al., 2009; Yanowitch, 1967].

[12] The f_oF_2 RMAs resulting from the removal of the solar cycle and intra-annual variability are presented in Figure 4a. The significant amount of remaining variability indicates that these terms do not fully account for the changing amplitude of the wave-4 longitudinal structure. The ONI values also shown in Figure 4a appear to correspond loosely with the values of the f_oF_2 RMAs. Although the agreement between the two is far from perfect, similar trends are observed in both. As the ONI values are representative of the ENSO, this indicates that changing atmospheric and oceanic circulations associated with the ENSO may be responsible for part of the variability in the wave-4 amplitude that is not associated with either solar cycle or intra-annual variability.

[13] To further explore the connection between the f_oF_2 RMAs and the ONI we have considered the yearly extreme values. The yearly extreme value (maximum or minimum with the sign maintained) of the ONI and the extreme value of the f_oF_2 RMA in the subsequent 5 months are shown in

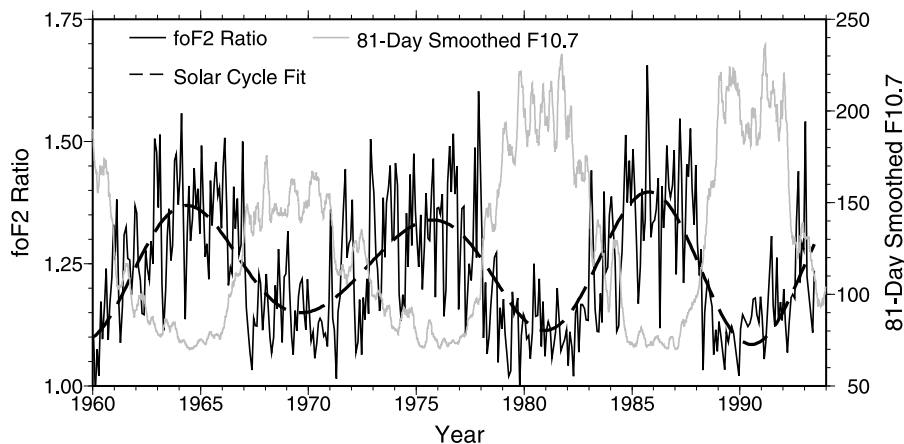


Figure 3. Ratio of the monthly median f_oF_2 value between the ionosonde stations in Maui and Yamagawa between 1500 and 1600 LT (solid black) from January 1960 to June 1993. The 81 day smoothed $F_{10.7}$ cm solar radio flux (grey) and the solar cycle fit (dashed black) are also shown.

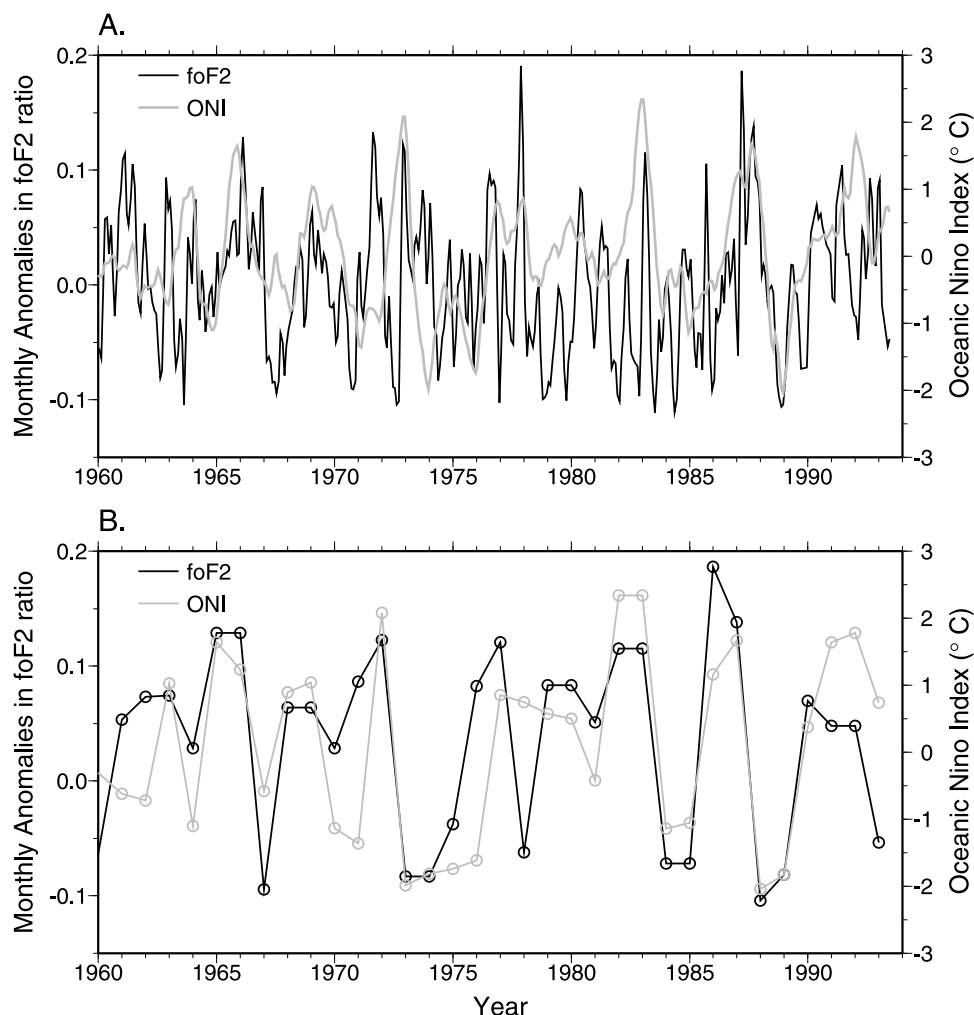


Figure 4. (a) Monthly f_oF_2 ratio anomalies (black) and ONI values (grey) from January 1960 to June 1993. (b) Yearly extreme value of ONI (grey) and the extreme value of f_oF_2 ratio anomalies in the subsequent 5 months (black).

Figure 4b. Changes in global surface temperature, precipitation, and outgoing longwave radiation can all lag behind changes in SSTs [Trenberth *et al.*, 2002], and it is necessary to consider any delay between SSTs and the ionospheric effect. We use the extreme value of the f_oF_2 RMA in the 5 months after the yearly extreme ONI value to account for any time delay and also any variation in the time delay. The results in Figure 4b demonstrate that significant increases or decreases in the ONI are related to similar increases or decreases in the f_oF_2 RMAs. The correlation coefficient between the yearly extreme values in ONI and f_oF_2 RMAs in the subsequent 5 months is 0.70 indicating good agreement between the two time series. This is a fascinating result and strongly suggests that changing SSTs associated with the ENSO are capable of influencing electron densities in the F region ionosphere. This surprising connection between the ENSO and the F region ionosphere reveals a new source of interannual ionospheric variability. As the f_oF_2 RMAs are thought to be representative of the wave-4 longitudinal structure, it is thought that the interannual variability in SSTs associated with the ENSO represents a source of interannual variability in the amplitude of the wave-4 longitudinal structure.

[14] The ENSO and associated atmospheric phenomenon occur quasi-periodically [Trenberth, 1976; Gu and Philander, 1994] and a wavelet analysis was performed to reveal if similar periodicities and occurrence times are present in the ONI values and the f_oF_2 RMAs. The wavelet power spectra computed using the Morlet waveform of the ONI and the f_oF_2 RMAs are shown in Figures 5a and 5b, respectively. To more clearly illustrate the relationship between the two wavelet power spectra, the ONI wavelet power spectra contours are overlaid onto the f_oF_2 RMA power spectra in Figure 5b. As can be seen in Figure 5, the ONI and f_oF_2 RMAs have similar periodicities and occurrence times. This provides further evidence for the possible connection between changing SSTs and the ionosphere wave-4 longitudinal structure.

[15] The results presented in Figures 4 and 5 demonstrate that the amplitude of the wave-4 longitudinal structure exhibits significant interannual variability and that this variability may be attributed in part to changing atmospheric and oceanic circulations associated with the ENSO. We now turn our attention to understanding how changing SSTs associated with the ENSO may introduce variability in the amplitude of the wave-4 longitudinal structure. Several

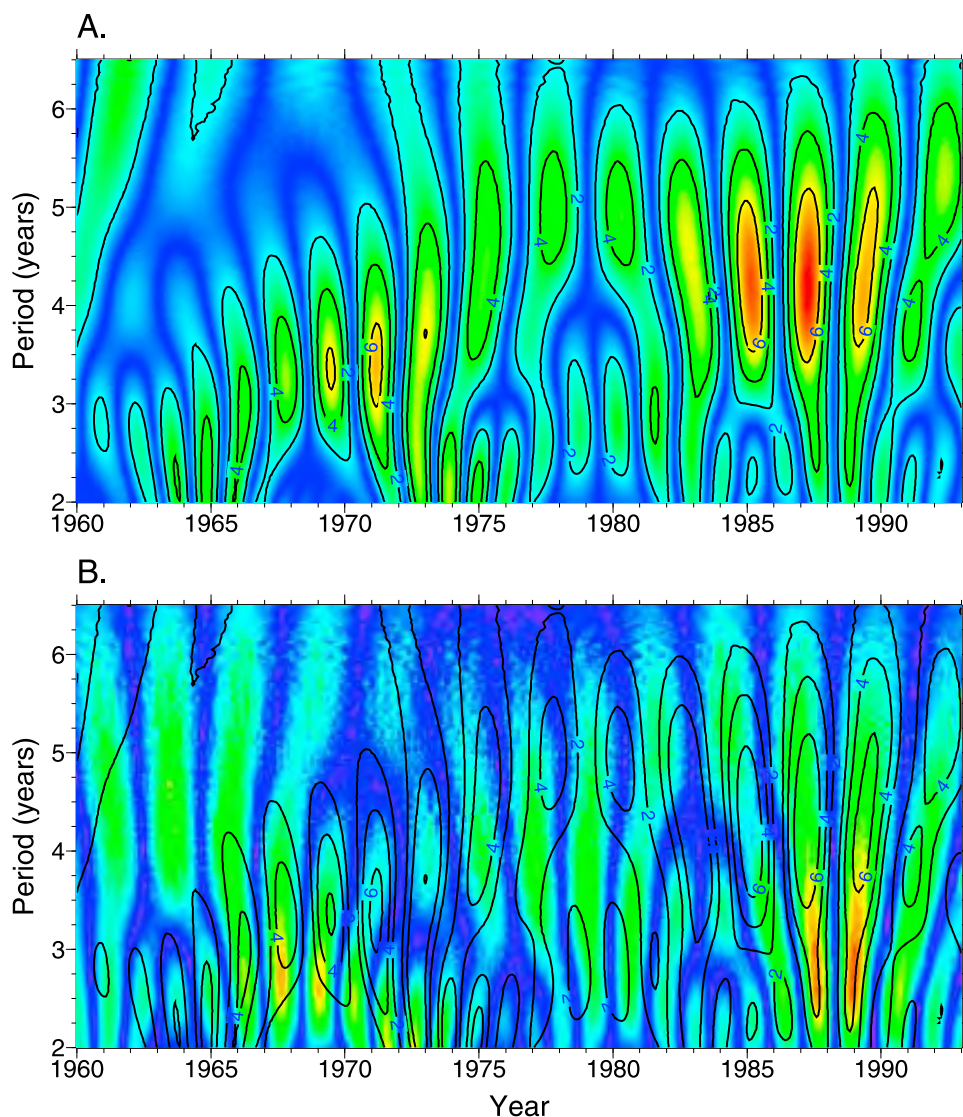


Figure 5. (a) Wavelet power spectra of the time series of ONI from January 1960 to June 1993. (b) Wavelet power spectra of the time series of monthly f_oF_2 ratio anomalies. The overlaid contours correspond to the ONI wavelet power spectra.

prior studies have revealed changes in tidal amplitudes in the lower atmosphere because of the ENSO. *Gurubaran et al.* [2005] hypothesized that an observed decrease in the amplitude of the diurnal tide in the mesosphere was due to an increase in the excitation of nonmigrating tides. Furthermore, a significant change in the latent heat forcing of nonmigrating tides over the equatorial region was observed during the 1997–1998 El Niño event [*Lieberman et al.*, 2007]. The complete spectrum of tidal amplitudes was observed to change with the largest changes being a decrease in the amplitude of DE3 and an increase in the amplitudes of DE1, DE2, DW3, and DW4. As DE3 is primarily responsible for generating the wave-4 longitudinal structure [*Hagan et al.*, 2007] a decrease in the amplitude of DE3 should reduce the strength of the wave-4 longitudinal structure. However, in the present analysis we observe an increase in the f_oF_2 RMAs (and presumably the wave-4 amplitude) in connection with periods of increased SSTs due to the ENSO. This discrepancy is most likely attributable

to the fact that the latent heating wave decompositions and interannual variabilities presented by *Lieberman et al.* [2007] were for a single latitude, namely, 2.5°S . As the first symmetric mode (Kelvin wave) of DE3 is of primary importance for modulating the E region dynamo fields [*Forbes et al.*, 2008], variations in DE3 heating at a single latitude do not unambiguously reveal how the amplitude of longitudinal structures in the ionosphere may change because of the ENSO. For instance, a decrease in DE3 heating amplitude at a single latitude could just as plausibly be produced by a latitudinal shift in structure as a uniform decrease in the amplitude of that structure. Thus, the most that we can conclude is that the forcing of nonmigrating tides is likely to be significantly affected by the ENSO, and that this is consistent with our hypothesis concerning the origins of wave-4 variability.

[16] Although the results in Figures 4 and 5 indicate a connection between the wave-4 longitudinal structure and changing SSTs, there are some time periods where the

relationship is not so apparent. There are several potential reasons for these discrepancies and future studies are necessitated to further explore how the ENSO influences longitudinal structures in the ionosphere. First, it remains unclear how the ENSO affects the generation of nonmigrating tides. In particular, the extent to which the ENSO influences the amplitude of symmetric mode of DE3 is not known. Future studies are required in order to understand both the significance of the changes in DE3 due to the ENSO and also the duration of these effects. Developing a comprehensive understanding of how the symmetric (Kelvin) mode of DE3 is influenced by the ENSO is fundamental to understanding the observed interannual variability in the wave-4 longitudinal structure. Another possible cause of the occasional disagreement between the wave-4 longitudinal structure and the ONI is the use of the f_oF_2 ratio as a proxy for the wave-4 amplitude. The f_oF_2 ratio may not perfectly reflect the wave-4 amplitude because of either shifting locations of the maxima and minima of the wave-4 structure or changes in the dominant longitudinal structure to wave-2 or wave-3. In the future, as the time series of global ionospheric measurements (such as GPS TEC and satellite measurements) lengthen, it will be possible to explore the interannual variability in the wave-4 longitudinal structure directly based on global observations.

4. Conclusions

[17] While previous studies have demonstrated the intra-annual variability in the longitudinal structure of the ionosphere [e.g., Liu and Watanabe, 2008; Pedatella et al., 2008; Scherliess et al., 2008; Wan et al., 2008], the present study has demonstrated that significant interannual variability is also present. Using the ratio of f_oF_2 between the ionosondes at Maui and Yamagawa as a proxy for the amplitude of the wave-4 longitudinal structure, we have demonstrated that the interannual variability is connected with changing SSTs associated with the ENSO. It is thought that the ENSO induces an interannual variability in the amplitude of nonmigrating tides which produces a similar interannual variability in the wave-4 longitudinal structure.

[18] The fact that changes in SSTs affect the ionosphere several hundred kilometers above the Earth's surface is a surprising new discovery and demonstrates the complex nature of the ocean-atmosphere-ionosphere system. Additional studies are necessary in order to develop a complete understanding of how changing SSTs influence longitudinal structures in the ionosphere. Of primary importance is how the generation of nonmigrating tides is influenced by the ENSO. Given the hypothesis that the interannual variability in the wave-4 longitudinal structure is due to interannual variability in the amplitude of DE3, one may further expect to observe significant day-to-day variability in the strength of the wave-4 longitudinal structure. Immel et al. [2009] demonstrated that significant day-to-day variability is present in the wave-4 longitudinal structure that is associated with day-to-day variability in DE3. Although the connection between changing tidal amplitudes in the lower atmosphere and longitudinal structures in the ionosphere is now well established, future studies are necessitated in order to reveal both the causes

of variability in the tidal amplitude and how these changes may influence longitudinal structures in the ionosphere.

[19] **Acknowledgments.** The authors wish to thank the providers of data used in the present study. This work was supported by NASA grant NNX08AF22G under the TIMED guest investigator program.

[20] Zuyin Pu thanks Subramanian Gurubaran and another reviewer for their assistance in evaluating this paper.

References

- Appleton, E. V. (1946), Two anomalies in the ionosphere, *Nature*, *157*, 691–693.
- Dow, J. M., R. E. Neilan, and G. Gendt (2005), The International GPS Service (IGS): Celebrating the 10th anniversary and looking to the next decade, *Adv. Space Res.*, *36*(3), 320–326, doi:10.1016/j.asr.2005.05.125.
- England, S. L., X. Zhang, T. J. Immel, J. M. Forbes, and R. DeMajistre (2009), The effect of non-migrating tides on the morphology of the equatorial ionospheric anomaly: seasonal variability, *Earth Planets Space*, *61*(4), 493–503.
- Forbes, J. M., and H. B. Garrett (1979), Theoretical studies of atmospheric tides, *Rev. Geophys.*, *17*, 1951–1981.
- Forbes, J. M., X. Zhang, and M. E. Hagan (2001), Simulations of diurnal tides due to tropospheric heating from the NCEP/NCAR Reanalysis Project, *Geophys. Res. Lett.*, *28*, 3851–3854.
- Forbes, J. M., J. Russell, S. Miyahara, X. Zhang, S. Palo, M. Mlynczak, C. J. Mertens, and M. E. Hagan (2006), Troposphere-thermosphere tidal coupling as measured by the SABER instrument on TIMED during July–September 2002, *J. Geophys. Res.*, *111*, A10S06, doi:10.1029/2005JA011492.
- Forbes, J. M., X. Zhang, S. Palo, J. Russell, C. J. Mertens, and M. Mlynczak (2008), Tidal variability in the ionospheric dynamo region, *J. Geophys. Res.*, *113*, A02310, doi:10.1029/2007JA012737.
- Gu, D., and S. G. H. Philander (1994), Secular changes of annual and interannual variability in the tropics during the past century, *J. Climate*, *8*, 864–876.
- Gurubaran, S., R. Rajaram, T. Nakamura, and T. Tsuda (2005), Interannual variability of diurnal tide in the tropical mesopause region: A signature of the El Niño–Southern Oscillation (ENSO), *Geophys. Res. Lett.*, *32*, L13805, doi:10.1029/2005GL022928.
- Hagan, M. E., and J. M. Forbes (2002), Migrating and nonmigrating diurnal tides in the middle and upper atmosphere excited by tropospheric latent heat release, *J. Geophys. Res.*, *107*(D24), 4754, doi:10.1029/2001JD001236.
- Hagan, M. E., A. Maute, R. G. Roble, A. D. Richmond, T. J. Immel, and S. L. England (2007), Connections between deep tropical clouds and the Earth's ionosphere, *Geophys. Res. Lett.*, *34*, L20109, doi:10.1029/2007GL030142.
- Hartman, W. A., and R. A. Heelis (2007), Longitudinal variations in the equatorial vertical drift in the topside ionosphere, *J. Geophys. Res.*, *112*, A03305, doi:10.1029/2006JA011773.
- Immel, T. J., E. Sagawa, S. L. England, S. B. Henderson, M. E. Hagan, S. B. Mende, H. U. Frey, C. M. Swenson, and L. J. Paxton (2006), Control of equatorial ionospheric morphology by atmospheric tides, *Geophys. Res. Lett.*, *33*, L15108, doi:10.1029/2006GL026161.
- Immel, T. J., S. L. England, X. Zhang, J. M. Forbes, and R. DeMajistre (2009), Upward propagating tidal effects across the E- and F-regions of the ionosphere, *Earth Planets Space*, *61*(4), 505–512.
- Kil, H., S.-J. Oh, M. C. Kelley, L. J. Paxton, S. L. England, E. Talaat, K.-W. Min, and S.-Y. Su (2007), Longitudinal structure of the vertical $\mathbf{E} \times \mathbf{B}$ drift and ion density seen from ROCSAT-1, *Geophys. Res. Lett.*, *34*, L14110, doi:10.1029/2007GL030018.
- Klobuchar, J. A. (1996), Ionospheric Effects on GPS, in *Global Positioning System: Theory and Applications*, vol. 1, *Prog. in Astronaut. and Aeronaut.*, vol. 163, edited by B. W. Parkinson and J. J. Spilker, pp. 485–515, Am. Inst. of Aeronaut. and Astronaut., New York.
- Lieberman, R. S., D. M. Riggan, D. A. Ortland, S. W. Nesbitt, and R. A. Vincent (2007), Variability of mesospheric diurnal tides and tropospheric diurnal heating during 1997–1998, *J. Geophys. Res.*, *112*, D20110, doi:10.1029/2007JD008578.
- Lin, C. H., W. Wang, M. E. Hagan, C. C. Hsiao, T. J. Immel, M. L. Hsu, J. Y. Liu, L. J. Paxton, T. W. Fang, and C. H. Liu (2007), Plausible effect of atmospheric tides on the equatorial ionosphere observed by the FORMOSAT-3/COSMIC: Three-dimensional electron density structures, *Geophys. Res. Lett.*, *34*, L11112, doi:10.1029/2007GL029265.
- Lindzen, R. S. (1970), Internal gravity waves in atmospheres with realistic dissipation and temperature, part I. Mathematical development and propagation of waves into the thermosphere, *Geophys. Fluid. Dyn.*, *1*, 303–355.

- Liu, H., and S. Watanabe (2008), Seasonal variation in the longitudinal structure of the equatorial ionosphere: does it reflect tidal influence from below?, *J. Geophys. Res.*, *113*, A08315, doi:10.1029/2008JA013027.
- Lühr, H., M. Rother, K. Hausler, P. Alken, and S. Maus (2008), The influence of nonmigrating tides on the longitudinal variation of the equatorial electrojet, *J. Geophys. Res.*, *113*, A08313, doi:10.1029/2008JA013064.
- Mannucci, A. J., B. D. Wilson, D. N. Yuan, C. H. Ho, U. J. Lindqwister, and T. F. Runge (1998), A global mapping technique for GPS-derived ionospheric total electron content measurements, *Radio Sci.*, *33*(3), 565–582.
- McDonald, S., K. F. Dymond, and M. E. Summers (2008), Hemispheric asymmetries in the longitudinal structure of the low-latitude nighttime ionosphere, *J. Geophys. Res.*, *113*, A08308, doi:10.1029/2007JA012876.
- Miyoshi, Y. (2006), Temporal variation of nonmigrating diurnal tide and its relation with the moist convective activity, *Geophys. Res. Lett.*, *33*, L11815, doi:10.1029/2006GL026072.
- Oberheide, J., Q. Wu, T. L. Killeen, M. E. Hagan, and R. G. Roble (2006), Diurnal nonmigrating tides from TIMED Doppler Interferometer wind data: Monthly climatologies and seasonal variations, *J. Geophys. Res.*, *111*, A10S03, doi:10.1029/2005JA011491.
- Oberheide, J., J. M. Forbes, K. Hausler, Q. Wu, and S. L. Bruinsma (2009), Tropospheric tides from 80 to 400 km: Propagation, interannual variability and solar cycle effects, *J. Geophys. Res.*, *114*, D00105, doi:10.1029/2009JD012388.
- Pedatella, N. M., J. M. Forbes, and J. Oberheide (2008), Intra-annual variability of the low-latitude ionosphere due to nonmigrating tides, *Geophys. Res. Lett.*, *35*, L18104, doi:10.1029/2008GL035332.
- Ropelewski, C. F., and M. S. Halpert (1987), Global and regional scale precipitation patterns associated with the El Nino/Southern Oscillation, *Mon. Weather Rev.*, *115*, 1606–1626.
- Sagawa, E., T. J. Immel, H. U. Frey, and S. B. Mende (2005), Longitudinal structure of the equatorial anomaly in the nighttime ionosphere observed by IMAGE/FUV, *J. Geophys. Res.*, *110*, A11302, doi:10.1029/2004JA010848.
- Scherliess, L., D. C. Thompson, and R. W. Schunk (2008), Longitudinal variability of low-latitude total electron content: Tidal influences, *J. Geophys. Res.*, *113*, A01311, doi:10.1029/2007JA012480.
- Smith, T. M., R. W. Reynolds, T. C. Peterson, and J. Lawrimore (2008), Improvements to NOAA's historical merged land-ocean surface temperature analysis (1880–2006), *J. Climate*, *21*, doi:10.1175/1007JCLI2100.1.
- Trenberth, K. E. (1976), Spatial and temporal variations of the Southern Oscillation, *Q. J. R. Meteorol. Soc.*, *102*, 639–653.
- Trenberth, K. E., J. M. Caron, D. P. Stepaniak, and S. Worley (2002), Evolution of El Nino–Southern Oscillation and global atmospheric surface temperatures, *J. Geophys. Res.*, *107*(D8), 4065, doi:10.1029/2000JD000298.
- Wan, W., L. Liu, X. Pi, M.-L. Zhang, B. Ning, J. Xiong, and F. Ding (2008), Wavenumber-4 patterns of the total electron content over the low latitude ionosphere, *Geophys. Res. Lett.*, *35*, L12104, doi:10.1029/2008GL033755.
- Xue, Y., T. M. Smith, and R. W. Reynolds (2003), Interdecadal changes of 30-yr SST normals during 1871–2000, *J. Climate*, *16*, 1601–1612.
- Yanowitch, M. (1967), The effect of viscosity on gravity waves and the upper boundary condition, *J. Fluid Mech.*, *29*, 209–231.

J. M. Forbes and N. M. Pedatella, Department of Aerospace Engineering Sciences, University of Colorado, 429 UCB, Boulder, CO 80309, USA. (forbes@colorado.edu; nicholas.pedatella@colorado.edu)